Influence of the Carrier-Envelope Phase of Few-Cycle Pulses on Ponderomotive Surface-Plasmon Electron Acceleration

S. E. Irvine,[1] P. Dombi,[2] Gy. Farkas,[2] and A. Y. Elezzabi[1]

[1]*Ultrafast Photonics and Nano-Optics Laboratory, Department of Electrical and Computer Engineering, University of Alberta, Edmonton, Alberta, Canada T6G 2V4*

[2]*Research Institute for Solid-State Physics and Optics, Hungarian Academy of Sciences, H-1121 Budapest, Konkoly-Thege M. út 29-33, Hungary*

(Received 13 April 2006; published 2 October 2006)

Control over basic processes through the electric field of a light wave can lead to new knowledge of fundamental light-matter interaction phenomena. We demonstrate, for the first time, that surface-plasmon (SP) electron acceleration can be coherently controlled through the carrier-envelope phase (CEP) of an excitation optical pulse. Analysis indicates that the physical origin of the CEP sensitivity arises from the electron's ponderomotive interaction with the oscillating electromagnetic field of the SP wave. The ponderomotive electron acceleration mechanism provides sensitive (nJ energies), high-contrast, single-shot CEP measurement capability of few-cycle laser pulses.

DOI: 10.1103/PhysRevLett.97.146801 PACS numbers: 73.20.Mf, 42.65.Re, 79.60.−i

New knowledge of fundamental light-matter interaction phenomena can be gained by controlling basic processes through the electric field of a light wave. The first experiments in this direction were enabled only recently by gaining control over the carrier-envelope phase (CEP) of few-cycle laser pulses [1]. For example, the generation of single isolated attosecond pulses [2,3] has resulted directly from the precise control over the CEP of few-cycle laser pulses used to generate the high-harmonic radiation. Moreover, it was observed [4] that the light waveform influences the harmonic generation process for much longer pulses (32 fs). Other bound-free electronic transition effects in gas-phase matter, including above-threshold ionization [5], indicate that the final velocity of electrons can be controlled through the CEP. Such results have had profound impact on various research fields [2,6] and further developments would lead to significant advancement in areas such as particle acceleration, high-harmonic generation from solids, and material science. Despite the vast amount of knowledge afforded by such investigations, significant progress has not been made in phase-related phenomena surrounding laser-solid interaction.

Of particular interest is the interaction of few-cycle pulses with metallic materials, *vis-à-vis* the behavior of conduction-band electrons in the vicinity of optical fields. Recent theoretical investigations [7] indicated that photoemission from a metallic surface would depend on the CEP and was later verified by experiments [8], although the effect was much smaller than originally predicted. Other pioneering research [9,10] has provided insight in the understanding of charge-carrier dynamics in semiconductor materials on a few femtosecond time scale.

Coherent control over the processes surrounding collective oscillations of the conduction electrons of a metal would provide a unique tool for many fields of research. The specific research area relevant to this study is the implementation of surface plasmons (SPs) for electron acceleration. We have demonstrated, through experimental and theoretical endeavors, that SPs are, in fact, capable of ponderomotive electron acceleration up to 2 keV [11,12] using many-cycle pulses. However, it is expected that the particular value of the CEP that the electron "sees" as it is born into the electromagnetic field will map directly onto the electron's final energy.

In this Letter, we demonstrate through model calculations that the ponderomotive energy gain experienced by an electron in the electric field of an SP wave can be controlled through the CEP. When the SP wave is excited with a few-cycle laser pulse, spectral shifts of the electron energy distributions are observed and are correlated with the specific form of the underlying electric field oscillation of the light wave. Thus, a method for coherent optical manipulation of the acceleration process is afforded through the CEP of the light field. Remarkably, the model indicates that this phenomenon would be observable even for optical pulses as long as 12 fs (~ 5 optical cycles), revealing a unique feature of this process among laser-solid interaction phenomena. Since SP generation and acceleration of electrons can be accomplished with only $\sim$1.5 nJ [13] excitation pulses, the technique opens a doorway into directly measuring the CEP of laser pulses available from typical laser oscillators, which is highly desired in other applications [14].

An ultrashort few-cycle laser pulse can be characterized by an electric field of the form $E_L(t, \varphi) = E_0(t)\cos(\omega t + \varphi)$, where $E_0(t)$ is the temporal envelope of the laser pulse, ω is the carrier frequency, and φ is the CEP of the electric field oscillation relative to the envelope peak $E_0(t = 0)$. In the most general situation, optically driven processes lack sensitivity to φ as $\tau_{\text{laser}} \gg T_0$, where τ_{laser} is the duration of the laser pulse and $T_0 = 2\pi/\omega$ is the period. However, cases where $\tau_{\text{laser}} \sim T_0$ provide the opportunity to study the

nature of SP-electron interaction on a time scale comparable to a single light-wave oscillation. The geometry for SP-electron acceleration is shown in Fig. 1(a). The few-cycle laser pulse is used to excite an SP wave at a metal surface. Coupling between the incident laser pulse and an SP mode localized at the metal-vacuum boundary is achieved through the Kretschmann configuration. The electromagnetic wave is resonantly absorbed and transformed into a longitudinal SP oscillation having an electric field described by the function: $E_{\mathrm{SP}}(z, t, \varphi) = \eta E_L(t, \varphi) \times \exp(-\gamma z)$, where η is the electric field enhancement factor and γ^{-1} is the characteristic penetration depth into vacuum. Because of this large enhancement, SP waves are well suited for studying electric field driven processes in matter. Typical values of these parameters are $\eta = 10^2$–10^3 and $\gamma^{-1} = 240$ nm (at a wavelength $\lambda = 800$ nm). More important, however, is the coherent impression of the CEP of $E_L(t, \varphi)$ onto the temporal structure of the plasmon wave and its subsequent effect on charged-particle acceleration. Photoelectrons, produced at the metallic surface during the same instant that the SP is launched, will be accelerated to considerable energies by the ponderomotive force resulting from the high-gradient E_{SP} [13]. The ponderomotive gain experienced by an electron is contingent upon the instantaneous value of E_{SP} during its photoinjection and subsequent interaction [12]; therefore, it is expected that the energies of the photo-accelerated electrons can be coherently controlled through the laser parameter φ.

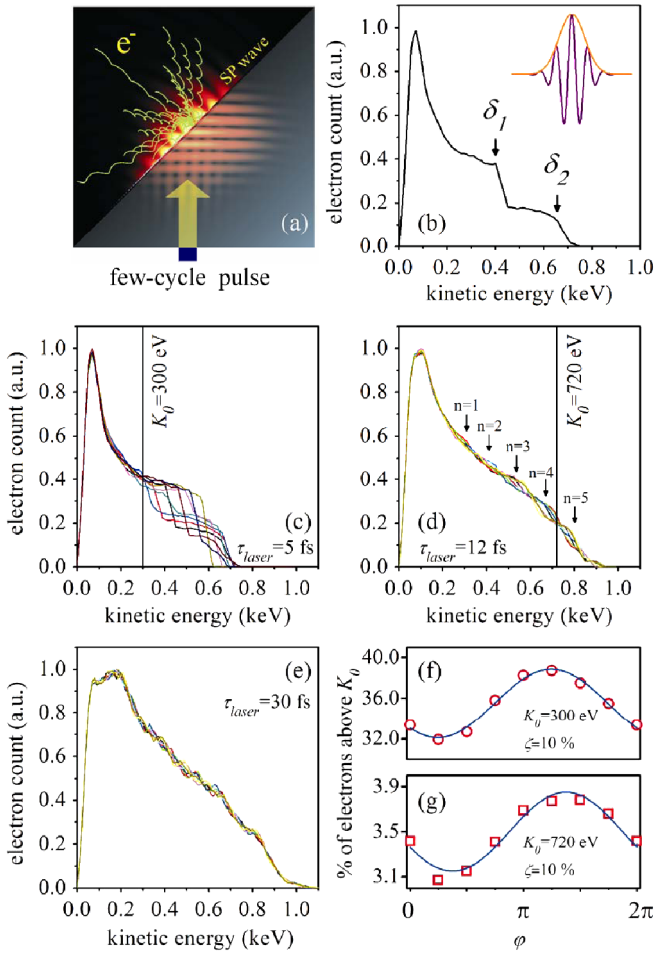

FIG. 1 (color online). (a) Illustration of the launching of an SP wave and subsequent dynamics of photoinjected electrons accelerated during the interaction with an SP wave excited with a $\tau_{\mathrm{laser}} = 5$ fs. (b) Calculated electron energy spectra for $\varphi = 0$ and $\tau_{\mathrm{laser}} = 5$ fs illustrating two pronounced cutoffs, positioned at values of $\delta_1 = 425$ eV and $\delta_2 = 685$ eV. Overlapped energy spectra of SP-accelerated electrons for φ ranging from 0 to 2π, and (c) $\tau_{\mathrm{laser}} = 5$ fs and (d) $\tau_{\mathrm{laser}} = 12$ fs. The arrows in (d) indicate regions of CEP sensitivity. Panel (e) illustrates overlapped energy spectra for $\tau_{\mathrm{laser}} = 30$ fs, which show no indication of CEP effects. Panels (f) and (g) illustrate the variation of the total number of electrons above $K_0 = 300$ eV and $K_0 = 720$ eV, respectively, which are also indicated by solid lines in (c) and (d).

Few-cycle SP acceleration involves a complex set of physical interactions including femtosecond electromagnetic pulse propagation, optical-plasmon coupling, electron photoemission from metallic surfaces, and free-electron dynamics in a vacuum dressed with E_{SP}. A generalized electrodynamic model should, indeed, incorporate all the aforementioned processes and allow for a complete description with respect to specific physical details concerning each of these interactions. In what follows, we shall describe the assumptions and motivations for the various components of our model. Finally, we implement this model to verify the influence of the CEP on SP-electron acceleration using a set of easily achievable experimental parameters.

SP-electron acceleration fundamentally arises from the ponderomotive interaction, which occurs between charged particles and an electromagnetic field gradient [12]. Therefore, the natural and most intuitive first step is to consider the spatial and temporal electromagnetic field distribution of an SP mode confined to the metal-vacuum boundary. To describe the electromagnetics we employ the numerical solution of Maxwell's equations: $\partial_t \vec{H} = -\mu_0^{-1} \nabla \times \vec{E}$ and $\partial_t \vec{E} = \varepsilon^{-1} \nabla \times \vec{H}$, where $\vec{H}$ is the magnetic intensity, $\vec{E}$ is the electric field (describing both E_{SP} and E_L), ε is the local permittivity, and μ_0 is the permeability of free space. For this, the finite-difference time-domain technique is used and is described sufficiently elsewhere [12,15].

Consideration must be also given to the photoejection mechanism of the conduction-band electrons of the metal film in the presence of the laser excitation, as the final ponderomotive energy gain is a strong function of the electron's initial position with respect to the accelerating E_{SP}. Numerous studies [11,16,17] indicate that, much like outer-shell electrons of atoms in an intense laser field, electrons in a metal film can experience either multiphoton bound-free transition or field emission, as determined by the Keldysh adiabaticity parameter γ [18]. It has been shown previously through density functional theory

(DFT) that the photoemission process itself can, in fact, depend upon the value of φ for the cases of $\gamma > 1$ or $\gamma < 1$ [7]. Marriage of such a DFT model with the electromagnetic description described above is possible, however, would require enormous computational effort as the two separate physical descriptions occur on completely different spatial scales (1 μm vs 0.1 nm). On the other hand, recent experiments [8] attempting to verify the DFT model for $\gamma > 1$ showed only a small variation ($< 0.1\%$) of electron count with φ. Therefore, we adopt the first-order assumption that the electronic charge emitted by the laser pulse is independent of the underlying waveform and follows the intensity of the laser pulse. While this assumption would no longer be valid in the cases where $\gamma < 1$, previous experiments [13,19] at laser-oscillator energies (nJ level) indicate that multiphoton absorption is the dominant photoemission mechanism, and therefore, we restrict our discussion to the nonadiabatic (multiphoton) $\gamma > 1$ regime. Hence, the rate of photoelectron generation is given by $\partial_t \rho(\vec{r}, t) \propto I^m_{\text{laser}}(\vec{r}, t)$, where $I^m_{\text{laser}}(\vec{r}, t)$ is the local intensity of the optical pulse and m is the order of the photoemission process. The trajectories of the photoemitted electrons, in response to E_{SP}, are calculated using the nonrelativistic momentum equation: $d_t \vec{v} = q m_e^{-1}(\vec{E} + \mu_0 \vec{v} \times \vec{H})$, where m_e and $\vec{v}$ are the mass and velocity of the electron, respectively. Within this formalism, Coulomb interaction between electrons is neglected, as the current density produced by photoemission (< 100 A/cm^2) is orders of magnitude less than the space-charge saturation value [12,13,20]. The wavelength of the optical excitation pulse is $\lambda_0 = 800$ nm and the metal film parameters are taken to be those of silver ($m = 3$) [13].

A calculated energy spectrum of SP-accelerated electrons is shown in Fig. 1(b) for $\tau_{\text{laser}} = 5$ fs, $\varphi = 0$, and a peak $E_{\text{SP}} = 1.8 \times 10^9$ V/cm (fluence of 1.5 nJ, spot size 60 μm [13]). Overall, the electron energy spectrum spans the range from 0 to 750 eV and contains a low-energy peak located at 70 eV. Two pronounced cutoffs, positioned at values of $\delta_1 = 425$ eV and $\delta_2 = 685$ eV, are clearly evident within the energy spectra. The origin of δ_1 and δ_2 is directly associated with the acceleration mechanism. For adiabatic ponderomotive forces, acceleration takes place over many cycles of the SP wave, and a photoinjected electron is allowed to "feel" many oscillations of the E_{SP}. Over time, the electron acquires a velocity that is proportional to the difference in the peak values of the subsequent electric field oscillations that the electron sees as it interacts with the SP field [21]. In such cases, where $\tau_{\text{laser}} \gg T_0$, the difference in neighboring peak electric field values is infinitesimal and translates into an equally incremental change in electron energy, ΔK. Depending on the time and location of emission into this field, an electron can accumulate a number of these discrete energy differences ranging from 0 to $n\Delta K$, where n is the number of electric field oscillations comprising the optical pulse. Since ΔK approaches zero for $\tau_{\text{laser}} \gg T_0$, the associated CEP effects will be insignificant. On the other hand, few-cycle SP acceleration is nonadiabatic in nature as ΔK is no longer infinitesimal. As the excitation optical pulse is delta-function–like, the electrons accelerated by the resultant SP wave will bear a signature of the underlying phase since ΔK is much larger as compared to the case of many-cycle pulses. The spectrum of Fig. 1(b) clearly exemplifies this situation. In this case $\tau_{\text{laser}} = 5$ fs, there are essentially only two periods ($n = 2$) at $\lambda = 800$ nm, which manifest themselves as δ_1 and δ_2 within the electron energy spectra.

To illustrate the dependence of energy of the SP-accelerated electrons on CEP, spectra having various values of φ are overlaid with each other and plotted in Fig. 1(c). While the spectra do not indicate any observable dependence on φ below energies of 200 eV, it is observed that the electron count above energy $K = 300$ eV (which represents $\sim$36% of the energy spectrum) has a marked dependence on φ. As shown in Fig. 1(f), for an energy range $K > K_0$ ($= 300$ eV), there is a clear sinusoidal relationship between the electron count, Q, and φ: $Q(K_0, \varphi) = A(K_0)\sin[\varphi + \varphi_0(K_0)] + Q_0$, where $\varphi_0(K_0)$ is the initial phase of the Q waveform for the energy range specified above K_0, $A(K_0)$ is the amplitude, and Q_0 is the baseline offset. Of particular interest is the contrast ratio, $\zeta = A(K_0)/Q_0$, which can be used as a figure of merit for the degree of CEP phase control. Shown in Fig. 1(f), we measure a significant $\zeta = 10\%$, corresponding to a change of 7% of the total number of electrons within the spectra.

Up to this point we have been considering two-cycle laser pulses ($\tau_{\text{laser}} \sim T_0$); to further demonstrate the phase sensitivity of the SP acceleration process at longer pulse durations, τ_{laser} is increased to 12 fs. Shown in Fig. 1(d) are the calculated electron energy distributions generated using $\tau_{\text{laser}} = 12$ fs for $\varphi = 0$ to 2π. Overall, each curve has the same characteristics of the spectra shown in Fig. 1(c). Since the longer τ_{laser} allows more interaction time between the photoinjected electrons and E_{SP}, the peak and maximum energy have up-shifted by 20% [12]. Despite the fact that we have used an optical pulse having $\tau_{\text{laser}} \sim 4.5T_0$, the electron energy distributions still exhibit a significant φ dependence. Careful inspection of the energy distributions reveal $n \sim 5$ distinct regions where the electron count changes significantly with the CEP, matching approximately the number of optical cycles in the 12 fs pulse. With the choice of a discrimination range $K_0 = 720$ eV, the sinusoidal $Q(K_0, \varphi)$ curve shown in Fig. 1(g) is obtained. Again, a contrast ratio of up to 10% is realized. However, owing to the increased pulse duration (and hence, less pronounced CEP effects), this sinusoidal variation accounts for $<1\%$ of the total number of electrons comprising the spectrum. As expected, when τ_{laser} is further increased to 30 fs, all indications of φ sensitivity vanish as evidenced by the indistinguishable overlapping electron energy spectra shown in Fig. 1(e).

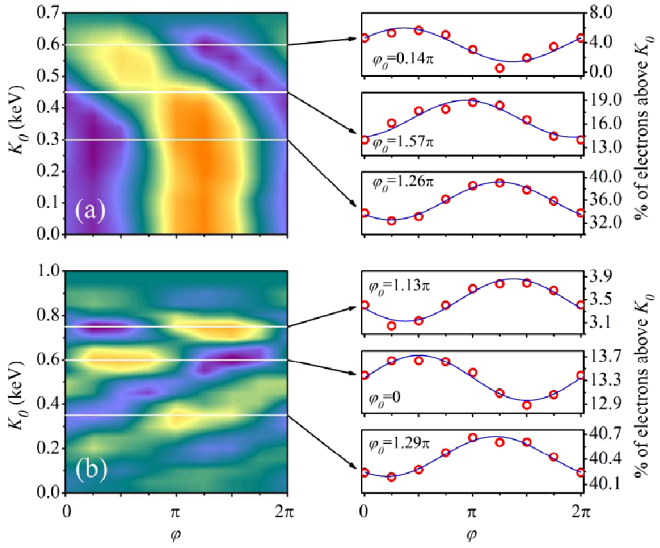

FIG. 2 (color online). $\Delta Q(K_0, \varphi)$ surface plots illustrating the electron count as a function of both K_0 and φ for (a) $\tau_{\text{laser}} = 5$ fs and (b) $\tau_{\text{laser}} = 12$ fs. Constant K_0 cross sections along surfaces are shown for both $\tau_{\text{laser}} = 5$ and 12 fs, indicating that $Q(K_0, \varphi)$ can be tailored to yield either sinelike or cosinelike waveforms.

To investigate the nature of the phase sensitivity and its relationship to electron energy, K_0 is continuously varied across the entire energy spectra of the SP-accelerated electrons. Figure 2(a) illustrates $\Delta Q(K_0, \varphi) = Q(K_0, \varphi) - Q_0$ and its variation with both K_0 and φ for $\tau_{\text{laser}} = 5$ fs. For a fixed φ, it is observed that $\Delta Q(K_0, \varphi)$ remains relatively constant as K_0 is varied from 0 to 300 eV. The lack of CEP sensitivity of the low-energy electrons [$<$ 300 eV, see Fig. 1(c)] is attributed to the fact that these electrons do not spend sufficient time interacting with E_{SP} field and/or are injected near the edges of the SP wave [12,22]. In either case, the underlying CEP is not imprinted onto those particular low-energy electrons. However, for the energy range 300 eV $< K_0 <$ 600 eV, $\varphi_0(K_0)$ differs by $\sim 1.1\pi$ and is manifested as a phase displacement of $\Delta Q(K_0, \varphi)$. Constant $K_0 = 300$, 450, and 600 eV cross sections along the $\Delta Q(K_0, \varphi)$ surface shown in Fig. 2(a) exemplify this phase shift. Over this energy range, only Q_0 and φ_0 are changing, while the amplitude $A(K_0)$ remains nearly constant. As K_0 continues to increase beyond 600 eV, $\varphi_0(K_0)$ is approximately constant, while $A(K_0)$ decreases to zero as the spectral components of the kinetic energy distribution vanish. The specific values of φ_0, Q_0, and A are intricately coupled to the exact position of K_0 with respect to dynamical δ_1 and δ_2. Evidently, it is possible to tailor K_0 to arrive at an optimal value of $\zeta(K_0) = 60\%$ at $K_0 = 600$ eV. It is also important to illustrate that a phase-sensitive $\Delta Q(K_0, \varphi)$ surface can be achieved for even longer duration optical pulses of $\tau_{\text{laser}} =$ 12 fs as shown in Fig. 2(b). Here, five distinct regions, corresponding to the number the optical cycles ($n \sim 5$), are evident in the phase-sensitive map. Examination of constant $K_0 = 350$, 600, and 750 eV cross sections along the $\Delta Q(K_0, \varphi)$ surface demonstrate that $Q(K_0, \varphi)$ can be either "sinelike" or "cosinelike"; however, the optimal $\zeta(K_0)$ is reduced to 10% for $K_0 = 750$ eV.

In summary, we have shown that SP-electron acceleration can be controlled directly through the CEP of a few-cycle optical pulse. Model calculations reveal that the phase-variation of the photoaccelerated electrons arises from their ponderomotive interaction with the electric field of the SP wave, and offers a method of optical control of the acceleration process through the CEP parameter. Coherent control over the processes surrounding collective oscillations of the conduction electrons of a metal is relevant to many fields of research. A potential short-term outcome is the application to direct CEP measurement of few-cycle laser pulses produced by laser-oscillator systems.

The authors are indebted to F. Krausz for his comments. This work is supported by the Natural Sciences and Engineering Research Council of Canada (NSERC), the Hungarian Scientific Research Fund (Projects No. T048324 and No. F60256), and the ULTRA COST P14 programme of the EU.

[1] D. J. Jones *et al.*, Science **288**, 635 (2000).
[2] P. Agostini and L. F. DiMauro, Rep. Prog. Phys. **67**, 813 (2004).
[3] A. Baltuska *et al.*, Nature (London) **421**, 611 (2003).
[4] G. Sansone *et al.*, Phys. Rev. Lett. **94**, 193903 (2005).
[5] G. G. Paulus *et al.*, Phys. Rev. Lett. **91**, 253004 (2003).
[6] S. T. Cundiff and J. Ye, Rev. Mod. Phys. **75**, 325 (2003).
[7] Ch. Lemell *et al.*, Phys. Rev. Lett. **90**, 076403 (2003).
[8] A. Apolonski *et al.*, Phys. Rev. Lett. **92**, 073902 (2004).
[9] T. M. Fortier *et al.*, Phys. Rev. Lett. **92**, 147403 (2004).
[10] O. D. Mücke *et al.*, Opt. Lett. **29**, 2160 (2004).
[11] S. E. Irvine and A. Y. Elezzabi, Appl. Phys. Lett. **86**, 264102 (2005).
[12] S. E. Irvine and A. Y. Elezzabi, Phys. Rev. A **73**, 013815 (2006).
[13] S. E. Irvine, A. Dechant, and A. Y. Elezzabi, Phys. Rev. Lett. **93**, 184801 (2004).
[14] P. Dombi *et al.*, New J. Phys. **6**, 39 (2004).
[15] A. Taflove, *Computational Electrodynamics* (Artech House, Boston, 1995).
[16] C. Tóth, Gy. Farkas, and K. L. Vodopyanov, Appl. Phys. B **53**, 221 (1991).
[17] L. A. Lompre, J. Thebault, and Gy. Farkas, Appl. Phys. Lett. **27**, 110 (1975).
[18] L. V. Keldysh, Sov. Phys. JETP **20**, 1307 (1965).
[19] T. Tsang, T. Srinivasan-Rao, and J. Fischer, Phys. Rev. B **43**, 8870 (1991).
[20] J. P. Girardeau-Montaut and C. Girardeau-Montaut, J. Appl. Phys. **65**, 2889 (1989).
[21] For example, see F. F. Chen, *Introduction to Plasma Physics and Controlled Fusion* (Plenum, New York, 1984), 2nd ed.
[22] J. Kupersztych, P. Monchicourt, and M. Raynaud, Phys. Rev. Lett. **86**, 5180 (2001).